

The effect of mirabilite precipitation on the absolute and practical salinities of sea ice brines

Butler, Benjamin; Papadimitriou, Efsthios; Kennedy, Hilary

Marine Chemistry

DOI:

[10.1016/j.marchem.2016.06.003](https://doi.org/10.1016/j.marchem.2016.06.003)

Published: 20/08/2016

Peer reviewed version

[Cyswllt i'r cyhoeddiad / Link to publication](https://doi.org/10.1016/j.marchem.2016.06.003)

Dyfyniad o'r fersiwn a gyhoeddwyd / Citation for published version (APA):

Butler, B., Papadimitriou, E., & Kennedy, H. (2016). The effect of mirabilite precipitation on the absolute and practical salinities of sea ice brines. *Marine Chemistry*, 184(August), 21-31. <https://doi.org/10.1016/j.marchem.2016.06.003>

Hawliau Cyffredinol / General rights

Copyright and moral rights for the publications made accessible in the public portal are retained by the authors and/or other copyright owners and it is a condition of accessing publications that users recognise and abide by the legal requirements associated with these rights.

- Users may download and print one copy of any publication from the public portal for the purpose of private study or research.
- You may not further distribute the material or use it for any profit-making activity or commercial gain
- You may freely distribute the URL identifying the publication in the public portal ?

Take down policy

If you believe that this document breaches copyright please contact us providing details, and we will remove access to the work immediately and investigate your claim.

The effect of mirabilite precipitation on the absolute and practical salinities of sea ice brines

Benjamin Miles Butler^a, Stathys Papadimitriou^a, Hilary Kennedy^a

^a*School of Ocean Sciences, Bangor University, Menai Bridge, Anglesey, LL59 5AB, UK*

Abstract

The sea ice cover of high latitude oceans contains concentrated brines which are the site of *in-situ* chemical and biological reactions. The brines become supersaturated with respect to mirabilite ($\text{Na}_2\text{SO}_4 \cdot 10\text{H}_2\text{O}$) below -6.4°C , and the associated removal of Na^+ and SO_4^{2-} from the brine results in considerable non-conservative changes to its composition. The changes are reflected in the brine salinity, which is a fundamental physico-chemical parameter in the sea ice brine system. Here, measurements of electrical conductivity and brine composition in synthetic sea ice brines between -1.8 and -20.6°C , obtained during a comprehensive investigation of the brine-mirabilite equilibrium at below-zero temperatures reported elsewhere, are combined with modelled estimates to assess the behaviour of the absolute (S_A) and practical (S_P) salinities of sea ice brines. Results display substantial divergence of S_P from S_A below -6.4°C , reaching a 7.2 % difference at -22.8°C . This is shown to create inaccuracies when S_P is assumed to be equivalent to S_A , firstly by misrepresenting the conditions inhabited by sea ice biota, whilst also creating errors in the calculation of physical sea ice parameters. Our measured and modelled data are used to refine the $S_A - T$ relationship for sea ice brines, implicit of mirabilite precipitation, which is crucial in estimat-

ing brine properties in absence of salinity data. Furthermore, because S_P is the parameter measured in field studies, we provide an $S_P - T$ relationship for sea ice brines to -22.8°C , which aids in explaining the trends observed in available $S_P - T$ data from sea ice brines in the Southern Ocean, demonstrating the importance of the mirabilite-brine equilibrium in natural sea ice. Finally, we initiate the development of a conversion factor for the estimation of S_A from S_P measurement in sea ice brines, and produce an equation that can calculate S_A from modelled brine density. This work ultimately highlights careful consideration of salinity concepts when applied to the sea ice system.

Keywords: Mirabilite, Sea ice, Salinity, FREZCHEM

1. Introduction

The Na–K–Mg–Ca–Cl–SO₄–H₂O system describes 99.4 % of the major dissolved ions in Standard Seawater by weight (Millero et al., 2008), and these ions have long been known to display constant ratios to one another throughout the world ocean (Forchhammer, 1865; Dittmar et al., 1873). This conservative behaviour gave rise to the concept of salinity, which was originally defined as a measure of the mass of dissolved salts per unit mass of seawater and is now termed absolute salinity (S_A) (Lewis, 1980). Accurate and rapid determination of salinity is paramount in the calculation of seawater density (Millero et al., 2008; Pawlowicz, 2015), therefore, since the advent of salinity as a concept, the method of its measurement has evolved to its present form of determination from measurement of electrical conductivity (Fofonoff, 1985; Lewis, 1980). The combined contribution of charged

14 dissolved species to the total electrical conductivity of a solution is a con-
 15 servative property and its measurement is converted to ‘practical’ salinity
 16 (S_P) by the Practical Salinity Scale 1978 (PSS-78). According to the PSS-78
 17 definition (Perkin and Lewis, 1980), the S_P of a solution is derived from the
 18 ratio (R_{15}) of the total electrical conductivity of the solution to that of a
 19 solution of potassium chloride (KCl) in pure water with a KCl mass fraction
 20 of 32.4356 g when both solutions are at 15 °C on the IPTS-68 scale, and zero
 21 gauge pressure (Fofonoff, 1985; Lewis, 1980; Millero et al., 2008). Practical
 22 salinity is dimensionless, and when $R_{15} = 1$, $S_P = 35$. The reproducibility
 23 of conductivity measurements is good enough for deep sea research where
 24 S_P accuracies within ± 0.006 (King et al., 2001) are required, and is now the
 25 dominant method for salinity measurement in both oceanography at sea and
 26 in the laboratory. Measurement of S_P also allows for precise calculation of S_A
 27 based on the most recent accurate chemical analysis defining $S_A = 35.16504$
 28 $\text{g kg}_{\text{solution}}^{-1}$ in Standard Seawater with $S_P = 35$ (Millero et al., 2008), with
 29 $S_A/S_P = 1.004715 \pm 0.0005$ (Jackett et al., 2006; Pawlowicz, 2012; Millero
 30 et al., 2008; Millero and Huang, 2009). This relationship is valid for practical
 31 salinities between 2 and 42, which is the working salinity range of the PSS-78
 32 (Lewis, 1980; Pawlowicz, 2012).

33 The electrical conductivity of a solution is a function of its temperature,
 34 the total amount of charged species dissolved in it, and their inter-ionic
 35 ratios (Weeks, 2010). Deviations from the constant stoichiometric ratios
 36 of Standard Seawater (table 1) will occur as a result of any process that
 37 leads to non-conservative behaviour of the major ions, with the formation of
 38 seawater-derived brines in evaporative or cryospheric environments providing

39 apt examples (McCaffrey et al., 1987; Marion et al., 1999; Grasby et al., 2013;
 40 Butler et al., 2016). Amongst the best studied cryospheric environments
 41 on Earth is the sea ice cover of high latitude oceans, which extends over
 42 approximately 20 million km² seasonally (Dieckmann and Hellmer, 2010),
 43 covering $\sim 5\%$ of the Earths surface. Sea ice undergoes large changes in
 44 temperature, chemical composition, and structure throughout its seasonal
 45 cycle (Gleitz et al., 1995), which are reflected in the labyrinth of inclusions
 46 within the ice that contain rejected liquid brine at local ice-brine (thermal)
 47 equilibrium (Weeks and Ackley, 1986; Petrich and Eicken, 2010; Light et al.,
 48 2003; Golden et al., 2007). At the low temperature (-1.8 to ~ -35 °C; Miller
 49 et al., 2011) and hypersaline conditions (up to ~ 220 g kg_{solution}⁻¹; Ewert and
 50 Deming, 2013) of sea ice brines, a suite of dissolved salts reach saturation
 51 with respect to their, typically hydrated, solid phases, which precipitate.
 52 The current understanding of solid-solution equilibria in sea ice states the
 53 following sequence of precipitates from sea ice brine as it cools to its eutectic:
 54 ikaite ($\text{CaCO}_3 \cdot 6\text{H}_2\text{O}$) at temperatures less than -2 °C (depending on brine
 55 $p\text{CO}_2$; Papadimitriou et al., 2013), mirabilite ($\text{Na}_2\text{SO}_4 \cdot 10\text{H}_2\text{O}$) at -6.4 °C
 56 (Butler et al., 2016), hydrohalite ($\text{NaCl} \cdot 2\text{H}_2\text{O}$) at -22.9 °C (Marion et al.,
 57 1999; Butler and Kennedy, 2015), sylvite (KCl) at -33 °C, and $\text{MgCl}_2 \cdot 12\text{H}_2\text{O}$
 58 at -36.2 °C (Gitterman, 1937; Nelson and Thompson, 1954). In addition
 59 to this sequence, gypsum ($\text{CaSO}_4 \cdot 2\text{H}_2\text{O}$) may also precipitate (Gitterman,
 60 1937; Marion et al., 1999), though estimates for the temperature region of
 61 its precipitation are conflicting, and range from -3 °C (Geilfus et al., 2013)
 62 to -22.2 °C (Marion et al., 1999).

63 Salt precipitation in sea ice can result in substantial non-conservative

64 changes in the ionic composition of the brine; recent measurements indicate
65 that mirabilite precipitation results in a reduction of the total concentrations
66 of Na^+ and SO_4^{2-} by up to 13 % and 92 %, respectively, by -20.6°C (Butler
67 et al., 2016). The changes are particularly significant given that these ions
68 contribute approximately 38 % to S_A (table 1) and 30 % to the total electrical
69 conductivity of the solution.

Table 1: A comparison of the compositions of Simplified (DOE, 1994) and Standard (Millero et al., 2008) Seawater. The remaining ions in Standard Seawater that are not tabulated include: Sr^{2+} , HCO_3^- , Br^- , CO_3^{2-} , B(OH)_4^- , F^- , OH^- , B(OH)_3 and CO_2 .

$S_P = 35$		
Solute	Simplified seawater	Standard Seawater
	$\text{g kg}_{\text{sol}}^{-1}$	
Na^+	10.7848	10.7815
K^+	0.3992	0.3991
Mg^{2+}	1.2840	1.2837
Ca^{2+}	0.4152	0.4121
Cl^-	19.4715	19.3527
SO_4^{2-}	2.7128	2.7124
H_2O	964.93	964.83
Remaining ions	N/A	0.2285

70 Salt precipitation in sea ice is confined to the brine inclusions that per-
71 meate its structure, ranging in diameter from $10\ \mu\text{m}$ to $10\ \text{mm}$ depending
72 on the ice temperature (Light et al., 2003). The physical and chemical prop-
73 erties of the brine define the conditions inhabited by the sympagic (within

ice) community, which is comprised of bacteria, microalgae, viruses, fungi, protozoans, and small metazoans (Horner et al., 1992; Thomas and Dieckmann, 2002; Ewert and Deming, 2013). Microscopic biota potentially covers between 6 and 41 % of the brine channel surface area at -2 °C (Krembs et al., 2000), while salt precipitates at colder temperatures may provide additional solid surfaces with which microorganisms can interact (Ewert and Deming, 2013). The salinity of the brine within the inclusions is temperature-dependent (Assur, 1960) and represents one of the major constraints on resident sea ice organisms because it affects the function of proteins and the surrounding osmotic conditions (Ewert and Deming, 2013). Brine salinities in sea ice extend from diluted seawater during ice melt with salinities <30 g $\text{kg}_{\text{solution}}^{-1}$, to salinities exceeding ~ 220 g $\text{kg}_{\text{solution}}^{-1}$ during winter months when the ice is at its coldest. For this reason, an accurate representation of brine salinity is required for determining the physico-chemical conditions of the internal sea ice habitat (Thomas et al., 2010; Ewert and Deming, 2013).

Sea ice salinity is most often measured as a bulk property, determined as S_P in melted sea ice samples. Measurements of bulk sea ice S_P are then used to estimate the physical parameters of the ice pack, such as brine volume fraction and porosity (Cox and Weeks, 1988; Gleitz et al., 1995; Petrich and Eicken, 2010). In such instances, the salinity of the internal brines can be estimated as S_A from the ice temperature via available liquidus equations (Assur, 1960; Cox and Weeks, 1986; Notz and Worster, 2009), assuming local ice-brine equilibrium, i.e., $T_{\text{ice}} = T_{\text{fr}}$, where T_{fr} = the freezing point of internal sea ice brine. These equations describe ice, water and salt mass balance as a function of temperature and are based on dissolved salt analysis

99 provided in the seminal work on seawater freezing by Nelson and Thompson
 100 (1954). The accuracy of the original measurements, with respect to mirabilite
 101 precipitation in particular, has recently been evaluated from a comprehensive
 102 assessment of mirabilite solubility in equilibrium sea ice brines (Butler et al.,
 103 2016). Discrepancies include indications for mirabilite-brine disequilibrium
 104 in the freezing experiments of Nelson and Thompson, and a warmer onset
 105 temperature of mirabilite precipitation (-6.4 °C) than previously thought
 106 (-8.2 °C). These discrepancies will be reflected in the liquidus ($S_A - T_{fr}$)
 107 equations for the ice-brine equilibrium (Assur, 1960; Cox and Weeks, 1986;
 108 Notz and Worster, 2009). In light of these recent developments, there is scope
 109 for refinement of the $S_A - T_{fr}$ relationship. In addition, while the liquidus
 110 equation in sea ice yields the S_A of the internal brines from ice temperature
 111 measurements, S_P is the property that is directly measured in sea ice brines
 112 as afforded by the available oceanographic instruments and protocols. Such
 113 brine samples are typically obtained by centrifugation or by drilling bore
 114 holes through the surface to varying depth in the ice (sackhole brines), and
 115 represent conditions that extend well into the temperature-salinity region
 116 of salt precipitation (Krembs et al., 2000; Papadimitriou et al., 2004; Munro
 117 et al., 2010; Norman et al., 2011; Garrison et al., 2003). Universally in sea ice
 118 research, the difference between brine S_A (from the liquidus equation) and S_P
 119 (as typically measured directly) is assumed to be insignificant or is ignored
 120 (Munro et al., 2010; Garrison et al., 2003; Norman et al., 2011). Therefore,
 121 there is also a pressing need for rigorous evaluation of the relevance of S_P
 122 measurements and of the S_A and S_P relationship in non-conservative sea ice
 123 brines.

Here, we examine the effect of salt precipitation on the practical and absolute salinities of synthetic sea ice brines at thermal equilibrium between -1.8 to -20.6 °C using laboratory measurements of S_A and S_P during an extensive investigation of the mirabilite-brine equilibrium at below-zero temperatures reported in Butler et al. (2016). In addition, we use the FREZCHEM thermodynamic code and equations for the electrical conductivity of individual ions (McCleskey et al., 2012) to model S_A and S_P in our experimental conditions. The FREZCHEM code has been developed for the study of cold aqueous geochemistry (Marion and Kargel, 2008) and has been used in the investigation of physical-chemical processes in sea ice (Marion et al., 1999; Grasby et al., 2013; Geilfus et al., 2013; Papadimitriou et al., 2013), and is particularly accurate in computing ice-brine-mirabilite equilibria in sea ice brines (Butler et al., 2016). Lastly, measured and modelled data are compared to $S_P - T$ data of natural sea ice brines from the Southern Ocean (Gleitz et al., 1995; Norman et al., 2011). Together the data are used; to assess and refine the existing $S_A - T_{fr}$ relationship compared to several empirical liquidus equations currently in use; to define a novel $S_P - T_{fr}$ relationship for sea ice brines implicit of mirabilite precipitation; develop a conversion factor that can account for the changing S_A to S_P ratio in sea ice brines affected by mirabilite precipitation; and to produce an empirical equation for the estimation of S_A from sea ice brine density.

145 2. Methods

146 2.1. Closed bottle incubations

147 A detailed account of the experimental protocol carried out for this inves-
148 tigation is provided in Butler et al. (2016). Synthetic brines were prepared
149 with the method of Kester et al. (1967) according to the composition of sim-
150 plified seawater (DOE, 1994) with respect to NaCl, KCl, MgCl₂, CaCl₂, and
151 Na₂SO₄ (table 1). Synthetic brines were used in order to simplify the pro-
152 tocol for the determination of S_A , requiring the measurement of 6 ions per
153 sample compared to the 14 per sample that would be required for natural
154 solutions (table 1). The brines were incubated in triplicate in screw-capped
155 (Teflon-lined) borosilicate media bottles at 2 °C below their estimated freez-
156 ing point according to the salinity/freezing-point relationship for seawater in
157 Millero and Leung (1976). The experimental temperatures ranged from -1.8
158 to -20.6 °C, with mirabilite being the only salt precipitate detected (by brine
159 analysis and synchrotron X-ray powder diffraction), forming at temperatures
160 ≤ -6.4 °C (Butler et al., 2016).

161 2.2. Measurement of absolute and practical salinities

162 The absolute salinity (S_A^{meas}) of the experimental solutions was obtained
163 by mass balance from measurement of the total ion concentrations in solution
164 (Na⁺, K⁺, Mg²⁺, Ca²⁺, Cl⁻, and SO₄²⁻). The Na⁺ and K⁺ concentrations
165 were determined by ion chromatography on a Dionex Ion Exchange Chro-
166 matograph ICS 2100. The Mg²⁺ and Ca²⁺ concentrations were determined
167 by potentiometric titration as described by Papadimitriou et al. (2013). The
168 Cl⁻ concentration was determined by gravimetric Mohr titration with 0.3 M

169 AgNO_3 standardized against NaCl purified by recrystallization. The SO_4^{2-}
 170 concentration was determined by precipitation as BaSO_4 in EDTA followed
 171 by gravimetric titration with MgCl_2 (Howarth, 1978). Repeat measurements
 172 of local seawater collected from the Menai Strait (53.1806°N , 4.2333°W) were
 173 used as an internal standard relative to the composition of Standard Seawa-
 174 ter (Millero et al., 2008). This comparison provided an estimate of accuracy
 175 of the measurements, which was 0.33 % for Na^+ , -0.97 % for K^+ , -0.36 %
 176 for Mg^{2+} , -0.39 % for Ca^{2+} , 0.48 % for Cl^- , and 0.35 % for SO_4^{2-} . The
 177 measured solution concentrations ($\text{mol kg}_{\text{sol}}^{-1}$) were converted to $\text{g kg}_{\text{sol}}^{-1}$ using
 178 the atomic masses provided by the International Union of Pure and Applied
 179 Chemistry (IUPAC). The $S_{\text{A}}^{\text{meas}}$ ($\text{g kg}_{\text{sol}}^{-1}$) was then calculated as follows:

$$S_{\text{A}} = \sum_{i=1}^n c_i MW_i \quad (1)$$

180 where the i^{th} of n constituents has a concentration of c_i ($\text{mol kg}_{\text{sol}}^{-1}$) and
 181 molecular mass MW_i (g mol^{-1}) (Pawlowicz, 2012). The combined analyti-
 182 cal and experimental errors yield an estimated accuracy of 0.22 % for $S_{\text{A}}^{\text{meas}}$,
 183 equivalent to $S_{\text{A}}^{\text{meas}} = 35.07$ at $S_{\text{A}} = 35.00 \text{ g kg}_{\text{sol}}^{-1}$. Note that our abso-
 184 lute salinity S_{A} is actually the Solution Absolute Salinity $S_{\text{A}}^{\text{soln}}$ of the new
 185 Thermodynamic Equation of Seawater - 2010 (IOC et al., 2010).

186 At present, there is no standard way of measuring practical salinities
 187 outside of the range specified in PSS-78, and in high salinity media, such
 188 as sea ice brines, samples are analysed by warming to laboratory tempera-
 189 ture followed by gravimetric dilution with pure water to values within the
 190 measurable range of PSS-78 (Pawlowicz, 2012; Norman et al., 2011; Gleitz
 191 et al., 1995; Papadimitriou et al., 2007). Here, practical salinity was mea-

192 sured (S_P^{meas}) using a portable conductivity meter (WTW Cond 3110) with a
 193 WTW Tetracon 325 probe at laboratory temperature ($20 - 26$ °C) following
 194 gravimetric dilution with distilled water to a target S_P of 35. The electrical
 195 conductivity (k) and, hence, the values of S_P^{meas} given by this instrument are
 196 automatically corrected to 25 °C (k_{25}). The conductivity meter was cali-
 197 brated in the $k_{25} = 10 - 95$ mS kg cm⁻¹ mol⁻¹ conductivity range, covering
 198 an S_P range of $10 - 70$, against a Guildline AUTOSAL oceanographic sali-
 199 nometer (instrument accuracy in $S_P = \pm 0.002$), itself calibrated with IAPSO
 200 Reference Seawater ($S_P = 35$). For this calibration we used local seawater
 201 ($S_P = 33 - 34$, assuming ionic ratios equivalent to Standard Seawater) and
 202 a range of diluted (with ultrapure MilliQ water) and concentrated (by freez-
 203 ing; Butler et al., 2016) solutions prepared from it. The S_P measured by this
 204 instrument can be described as a second order polynomial function of k_{25}
 205 ($R^2 = 0.9998$, $n = 336$, $p = < 0.001$), where

$$S_P = -0.039056 + 0.572499k_{25} + 0.001589k_{25}^2 \quad (2)$$

206 with an estimated standard error of ± 0.14 . Lastly, the S_P measured by the
 207 conductivity meter was multiplied by the dilution factor to obtain S_P^{meas} .

208 *2.3. Prediction of absolute salinity with FREZCHEM*

209 Using the chemical composition of our synthetic brines and enabling only
 210 the formation of ice and mirabilite in its solid phase database, the thermody-
 211 namic code FREZCHEM (Marion and Kargel, 2008; Marion et al., 2010) was
 212 used to model the absolute salinity (S_A^{mod}) of equilibrium sea ice brines. The
 213 code was run in 0.1 °C steps between -1.8 and -22.8 °C, and ion concentra-
 214 tions from the output were retrieved at each temperature. The temperature

215 minimum of the model run is beyond that covered by the laboratory experi-
 216 ments (-20.6 °C) and covers the full temperature range in which mirabilite
 217 is the major salt precipitate affecting brine composition in sea ice (Marion
 218 et al., 1999; Butler and Kennedy, 2015). In order to calculate S_A^{mod} using
 219 equation 1, the molal ($\text{mol kg}_{\text{H}_2\text{O}}^{-1}$) concentrations of the code output were
 220 converted to $\text{mol kg}_{\text{sol}}^{-1}$ by

$$\text{mol kg}_{\text{sol}}^{-1} = m \left(\frac{1000}{1000 + \sum_i m_i MW_i} \right), \quad (3)$$

221 where m_i and MW_i are the molality and molecular mass (g mol^{-1}) of the i^{th}
 222 ion in solution, respectively (Marion and Kargel, 2008).

223 The FREZCHEM code is based on the specific ion interaction model of
 224 electrolyte theory as formalized by Pitzer (1973). The Pitzer formalism has
 225 been found to account fully for ion-ion interactions except for those which
 226 exhibit large ion pair formation constants (He and Morse, 1993). For the syn-
 227 thetic brine compositions that were modelled, FREZCHEM explicitly com-
 228 puted the concentrations of HSO_4^- and MgOH^+ in addition to the unpaired
 229 major ions. Concentrations did not exceed $10^{-6} \text{ mol kg}_{\text{sol}}^{-1}$ for MgOH^+ and
 230 $10^{-9} \text{ mol kg}_{\text{sol}}^{-1}$ for HSO_4^- throughout the conditions of this study, rendering
 231 their contribution to S_A^{mod} negligible.

232 2.4. Modelling practical salinity with ionic molal conductivities

233 Because our S_P^{meas} is based on the total electrical conductivity measured
 234 in the synthetic brines as k_{25} , the same property was modelled (S_P^{mod}) using
 235 equations from McCleskey et al. (2012). The S_P^{mod} was calculated for the
 236 same chemical composition as the brines from the FREZCHEM modelling,

whilst ensuring that the conductivity calculations were carried out within their specified ionic range (McCleskey et al., 2012). The contribution of HSO_4^- and MgOH^+ to total electrical conductivity cannot be calculated using these equations, and again were considered negligible on account of their very low concentrations. The chemical composition of the brines extracted from the FREZCHEM model were normalised to an ionic strength of 0.72 mol $\text{kg}_{\text{H}_2\text{O}}^{-1}$ by the required dilution factor using a solver routine in Microsoft Excel. This dilution step was employed in order to replicate our experimental procedures. The electrical conductivity of each ion i in the solution at 25 °C was calculated by

$$k_{25,i} = \lambda_i m_i \quad (4)$$

where λ_i is the ionic molal conductivity and m_i is the ion molality. The λ_i is calculated as a function of ionic strength (I , molal) and temperature T (°C) by

$$\lambda_i = \lambda^\circ(T) - \frac{A(T)I^{0.5}}{1 + BI^{0.5}} \quad (5)$$

where B is an empirical constant, while λ° and A are functions of temperature described by the equations given in table 2. The ionic strength was calculated using

$$I = 0.5 \sum m_i z_i^2 \quad (6)$$

where z_i is the charge of the i^{th} ion.

The ionic molal conductivities of each ion calculated from equations 4 to 6 were summed to give the total electrical conductivity of the solution at 25 °C (k_{25}). Solution conductivities ($\text{mS kg cm}^{-1} \text{ mol}^{-1}$) were then converted to S_{p} according to equation 2, and were multiplied by the dilution factor to attain the undiluted $S_{\text{p}}^{\text{mod}}$ of the brine.

Table 2: Equations and constants from McCleskey et al. (2012) used for calculating λ° , A and B for use in equation 5, where T is temperature ($^\circ\text{C}$).

Ion	λ°	A	B
Na^+	$0.003763T^2 + 0.877T + 26.23$	$0.00027T^2 + 1.1410T + 32.07$	1.7
K^+	$0.003046T^2 + 1.261T + 40.70$	$0.00535T^2 + 0.9316T + 22.59$	1.5
Mg^{2+}	$0.010680T^2 + 1.695T + 57.16$	$0.02453T^2 + 1.9150T + 80.50$	2.1
Ca^{2+}	$0.009645T^2 + 1.984T + 62.28$	$0.03174T^2 + 2.3340T + 132.3$	2.8
Cl^-	$0.003817T^2 + 1.337T + 40.99$	$0.00613T^2 + 0.9469T + 22.01$	1.5
SO_4^{2-}	$0.010370T^2 + 2.838T + 82.37$	$0.03324T^2 + 5.8890T + 193.5$	2.6

2.5. Comparison with natural sea ice brine salinities

Our measured and modelled practical and absolute salinities were compared to available sea ice brine salinity data from Gleitz et al. (1995) and Norman et al. (2011). The two studies contain measurements of S_p for sea ice brines that were extracted through drainage into sack-holes. The field dataset spans a brine temperature range from -1.3 to -12.4 $^\circ\text{C}$, with S_p ranging from 29 to 179. All samples were taken from the seasonal ice zone of the Southern Ocean between 1991 and 2007.

3. Results

Both S_A^{meas} and S_p^{meas} increase at nearly identical rates down to -6.4 $^\circ\text{C}$ as increasing quantities of pure water are removed as ice to maintain thermal equilibrium (figure 1). In these experimental brines with a conservative composition, $S_A^{\text{meas}}/S_p^{\text{meas}} = 0.9995 \pm 0.0035$, which is 0.52 % lower than the value of 1.004715 ± 0.0005 in Standard Seawater (Millero et al., 2008; Jack-

ett et al., 2006). This difference is not significant ($p > 0.05$ as tested with
a two-tailed t-test with unequal variance), and we attribute it to the use
of simplified synthetic seawater composed of 6 major ions (table 1). Below
 -6.4 °C, S_P^{meas} increases at a greater rate than S_A^{meas} , coincident with the
redistribution of ions consequent of mirabilite precipitation. By -20.6 °C,
 S_P^{meas} is 5.7 % higher than S_A^{meas} , which results in $S_A^{\text{meas}}/S_P^{\text{meas}}$ reducing from
0.9995 to 0.9458.

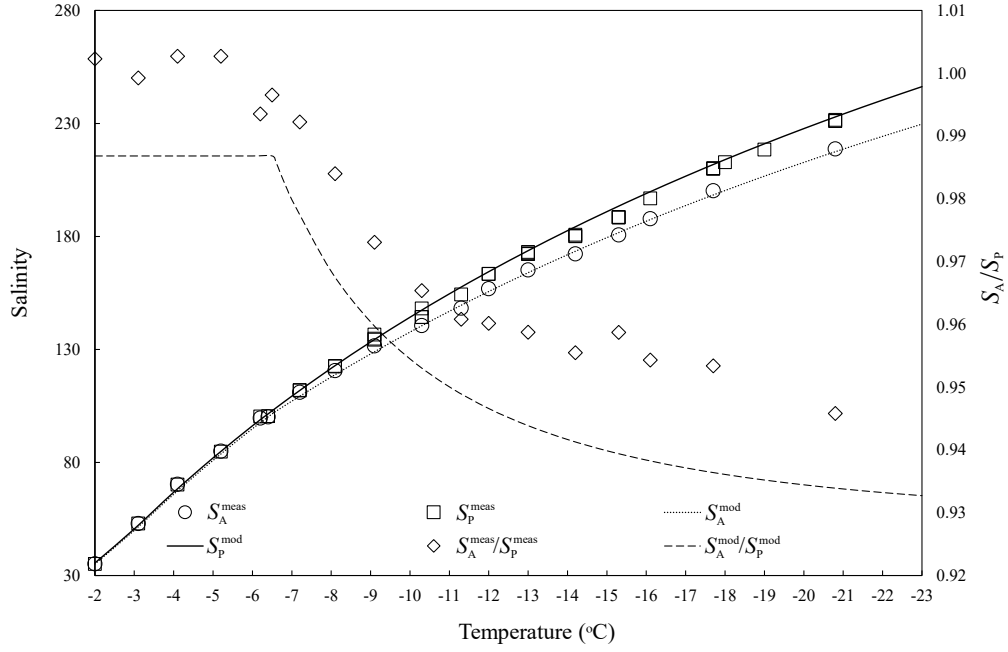


Figure 1: Measured and modelled S_A and S_P of equilibrium sea ice brines between -1.8 and -22.8 °C, and the associated S_A/S_P . The error of the measurements is within the diameter of the symbols.

Measured and modelled data displayed good agreement (figure 1). The
average difference between S_A^{mod} and S_A^{meas} was 0.89 ± 1.30 %, while that

282 between S_P^{mod} and S_P^{meas} was -0.62 ± 1.36 %, resulting in $S_A^{\text{mod}}/S_P^{\text{mod}}$ being
 283 consistently lower than that derived from our measurements by 0.014 ± 0.003 .
 284 Modelled brines at temperatures above -6.4 °C display an $S_A^{\text{mod}}/S_P^{\text{mod}} =$
 285 0.9868 , which reduces to 0.9327 at -22.8 °C when S_P^{mod} is 7.4 % higher than
 286 S_A^{mod} .

287 Whilst the S_P^{mod} has inherent inaccuracies (McCleskey et al., 2012), its
 288 agreement with the measurements allows its use as a means to assess the
 289 changes in the relative contribution of each major ion to the total electrical
 290 conductivity of the brines and, hence, S_P . A likewise evaluation can be done
 291 with respect to S_A using S_A^{mod} (table 3). The decrease in $S_A^{\text{mod}}/S_P^{\text{mod}}$ at tem-
 292 peratures below -6.4 °C (figure 1) is due to compositional changes in the
 293 brine relating to the removal of Na^+ and SO_4^{2-} from solution to mirabilite,
 294 as well as water in the mirabilite hydration water molecules. The largest
 295 decrease in percent contribution to solution conductivity and, hence, S_P^{mod} ,
 296 is that of SO_4^{2-} during its removal from solution to mirabilite (table 3). The
 297 change in percent contribution of Na^+ during the same process is less pro-
 298 nounced because of its 16.6 times larger background concentration (Millero
 299 et al., 2008). As a result, the contribution of the remaining ions to the elec-
 300 trical conductivity and S_P^{mod} increases accordingly. For all ions other than
 301 Na^+ , the change in percent contribution to S_A^{mod} is greater than that to S_P^{mod} ,
 302 but it is the overall redistribution of the ion contributions that affects the
 303 $S_A^{\text{mod}}/S_P^{\text{mod}}$ relationship observed (figure 1). The overall effect of the redistri-
 304 bution of ions (table 3) on S_A^{mod} and S_P^{mod} was hence tested according to their
 305 modelled outputs at a normalised ionic strength of $0.72 \text{ mol kg}_{\text{H}_2\text{O}}^{-1}$ (figure 2).
 306 The trends at normalised ionic strength indicate that changes induced by

307 mirabilite precipitation between -6.4 and -22.8 °C display a lesser overall
308 effect on S_A^{mod} than S_P^{mod} , both increasing in salinity by $0.3 \text{ g kg}_{\text{sol}}^{-1}$ and 2.3 ,
309 respectively.

310 It is important to note the absence of ikaite and gypsum from our exper-
311 iments, both of which have been identified in natural and synthetic sea ice
312 (Dieckmann et al., 2008; Geilfus et al., 2013; Fischer et al., 2013). Ikaite pre-
313 cipitation would not occur in the synthetic brines used for this investigation
314 due to the absence of CO_3^{2-} , its precipitation from sea ice brines is under-
315 stood to be a function of brine temperature and brine $p\text{CO}_2$, the latter as
316 an agent for the extent of ikaite saturation (Papadimitriou et al., 2013). The
317 maximum total dissolved Ca^{2+} concentration change at brine-ikaite equilib-
318 rium has been measured to be 4 % during its precipitation in cryogenic brines
319 to -7.5 °C (Papadimitriou et al., 2013). With respect to gypsum, the avail-
320 able scientific literature about its dynamics in sea ice contains inconsistent
321 findings (Gitterman, 1937; Nelson and Thompson, 1954; Marion et al., 1999;
322 Geilfus et al., 2013) and the potential extent of its precipitation from sea
323 ice brines between -1.8 and -22.8 °C is largely undefined experimentally.
324 The FREZCHEM code was therefore used to estimate the potential extent
325 of gypsum precipitation in sea ice within this temperature range, and yielded
326 maximum changes in total Ca^{2+} concentration of 10 %, with equimolar SO_4^{2-}
327 removal.

328 Whilst it is currently difficult to know the true extent of ikaite and gyp-
329 sum precipitation from sea ice brines, we used the higher estimates for their
330 potential effects on brine composition to estimate the associated changes to
331 S_A^{mod} and S_P^{mod} (using the same principles outlined in sections 2.3 and 2.4).

Table 3: The % contributions of the 6 constituent ions to S_A^{mod} and S_P^{mod} from conservative simplified seawater (DOE, 1994), to a sea ice brine at ice-brine-mirabilite equilibrium at -22.8 °C at 2 °C resolution.

T	$\%S_A^{\text{mod}}$						$\%S_P^{\text{mod}}$					
	Na ⁺	K ⁺	Mg ²⁺	Ca ²⁺	Cl ⁻	SO ₄ ²⁻	Na ⁺	K ⁺	Mg ²⁺	Ca ²⁺	Cl ⁻	SO ₄ ²⁻
Conserv.	30.754	1.138	3.662	1.184	55.525	7.737	26.435	1.091	6.317	1.291	61.394	3.472
-6.8	30.731	1.155	3.715	1.202	56.340	6.857	26.254	1.100	6.371	1.302	61.914	3.058
-8.8	30.663	1.203	3.869	1.252	58.673	4.341	25.746	1.126	6.520	1.333	63.372	1.903
-10.8	30.625	1.229	3.953	1.279	59.947	2.967	25.476	1.140	6.600	1.349	64.146	1.289
-12.8	30.603	1.245	4.004	1.295	60.719	2.134	25.315	1.148	6.648	1.359	64.609	0.922
-14.8	30.588	1.255	4.037	1.306	61.223	1.591	25.210	1.153	6.679	1.365	64.908	0.684
-16.8	30.578	1.262	4.060	1.313	61.569	1.218	25.139	1.157	6.699	1.369	65.112	0.523
-18.8	30.571	1.267	4.076	1.319	61.816	0.951	25.089	1.160	6.714	1.372	65.271	0.408
-20.8	30.565	1.271	4.083	1.322	61.998	0.755	25.052	1.162	6.725	1.375	65.364	0.323
-22.8	30.562	1.274	4.097	1.325	62.134	0.607	25.024	1.163	6.734	1.376	65.443	0.260

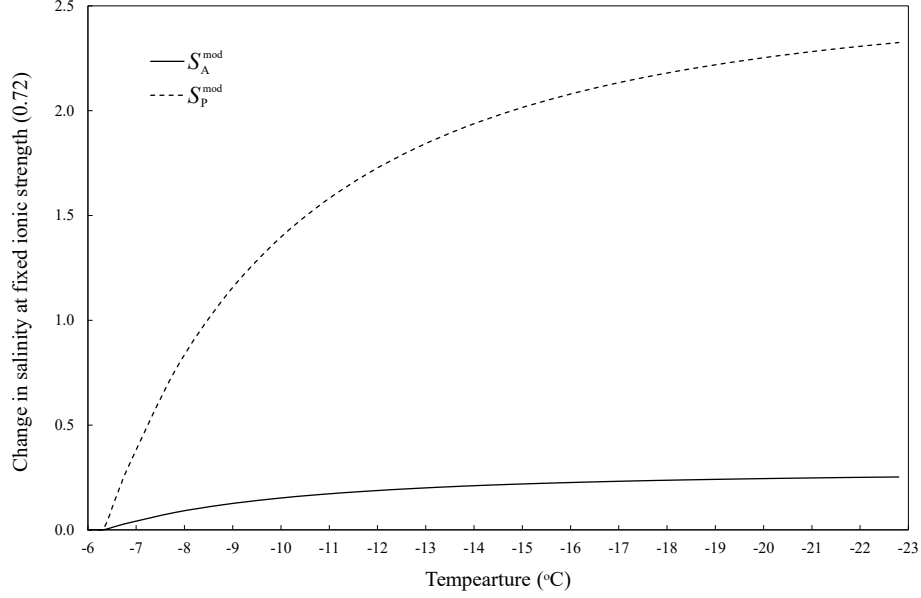


Figure 2: The change in S_A^{mod} and S_P^{mod} as a function of temperature, when the ionic strength of the brines are normalised by dilution to $0.72 \text{ mol kg}_{\text{H}_2\text{O}}^{-1}$.

332 Ikaite precipitation increased the difference between S_A^{mod} and S_P^{mod} by up
333 to 0.02 at -22.8°C . Gypsum precipitation showed more notable effects, in-
334 creasing the difference between S_A^{mod} and S_P^{mod} by up to 0.57 at -22.8°C .
335 Compared to the effects of mirabilite, which causes S_P^{mod} to exceed S_A^{mod} by
336 16.57 at -22.8°C , the potential contribution of ikaite and gypsum to the
337 observed salinities presented here are relatively minimal. Nonetheless it is
338 evident that ikaite and gypsum precipitation could further contribute to de-
339 viations between S_P and S_A in natural sea ice brines.

340 4. Discussion

341 4.1. The absolute salinity–temperature relationship in sea ice brines

342 Phase equations of sea ice, including the $S_A - T_{\text{fr}}$ relationship of sea
343 ice brines at thermal equilibrium, are a common tool for estimating brine
344 salinities when only temperature or bulk data is available (Cox and Weeks,
345 1986; Cox and Weeks, 1988; Garrison et al., 2003; Ewert and Deming, 2013;
346 Collins et al., 2008). For this reason, accurate and up to date equations are
347 a prerequisite for estimating the brine salinity reliably, and hence defining
348 one of the key environmental constraints imposed upon sympagic biota.

349 The most comprehensive assessment to date of the $S_A - T_{\text{fr}}$ relationship of
350 sea ice brines at thermal equilibrium is that of Assur (1960), who used major
351 ion measurements (Na^+ , K^+ , Mg^{2+} , Ca^{2+} , Cl^- and SO_4^{2-}) in frozen seawater
352 from Nelson and Thompson (1954), to deduce empirical equations from salt,
353 water and ice mass balance. Assur (1960) used two discrete functions to
354 describe the $S_A - T_{\text{fr}}$ relationship of sea ice brine, which converged at -8°C ,
355 the temperature at which mirabilite precipitation was understood to initiate
356 (Nelson and Thompson, 1954). Since 1960, Cox and Weeks (1986) and Notz
357 and Worster (2009) have simplified the two original functions by fitting the
358 same data to single polynomials for use in sea ice models (figure 3, top).

359 Our values of S_A^{mod} are derived from synthetic sea ice brines with a simpli-
360 fied ionic composition (table 1), which may introduce a slight bias compared
361 to the more complex composition of natural seawater (table 1). Despite this,
362 the ions included in the composition account for 99.4 % of the total S_A of
363 Standard Seawater (Millero et al., 2008), and the 0.6 % difference is within
364 the estimated error of S_A^{meas} . This reflects the accuracy of FREZCHEM in

describing Na^+ and SO_4^{2-} equilibria in sea ice brines as outlined in Butler et al. (2016). For these reasons, we use $S_{\text{A}}^{\text{mod}}$ between -1.8 and -22.8 °C to refine the $S_{\text{A}} - T_{\text{fr}}$ relationship of sea ice brines, implicit of the most recent understanding of mirabilite precipitation (Marion et al., 1999; Butler et al., 2016), to be:

$$S_{\text{A}}(T_{\text{fr}}) = 2.2330 - 19.3188T_{\text{fr}} - 0.6574T_{\text{fr}}^2 - 0.0110T_{\text{fr}}^3 \quad (7)$$

$$T_{\text{fr}}(S_{\text{A}}) = -0.174808 - 0.044057S_{\text{A}} - 1.08933 \times 10^{-4}S_{\text{A}}^2 - 5.54349 \times 10^{-7}S_{\text{A}}^3, \quad (8)$$

where T_{fr} is the brine freezing point (°C) and S_{A} is in $\text{g kg}_{\text{sol}}^{-1}$. Regressions used to derive equations 7 and 8 (and equations hereafter) were computed using the Data Analysis Toolpak in Microsoft Excel, with error values (σ) representing the standard error of the fit ($S_{\text{A}}(T_{\text{fr}})$: $R^2 = 0.9998$, $\sigma = 0.807$, $n = 211$, $p < 0.001$; $T_{\text{fr}}(S_{\text{A}})$: $R^2 = 0.99995$, $\sigma = 0.044$, $n = 211$, $p < 0.001$). We propose these equations for sea ice brines between -1.8 and -22.8 °C at brine-ice and brine-ice-mirabilite equilibrium. At -22.9 °C and below, hydrohalite precipitation results in further changes in brine composition and ionic ratios, and, therefore, an investigation of brine S_{A} and S_{P} below this temperature would require additional consideration of hydrohalite dynamics (Marion et al., 1999; Light et al., 2009; Butler and Kennedy, 2015).

Our refined $S_{\text{A}} - T_{\text{fr}}$ relationship generally corresponds well with the equations of Assur (1960), Cox and Weeks (1986), and Notz and Worster (2009) (figure 3, top). Major differences are seen around the temperature at which mirabilite begins to precipitate in sea ice, which recent investigation determined to occur at -6.4 °C (Butler et al., 2016) rather than the previously thought temperature of -8.2 °C (Nelson and Thompson, 1954; Assur, 1960).

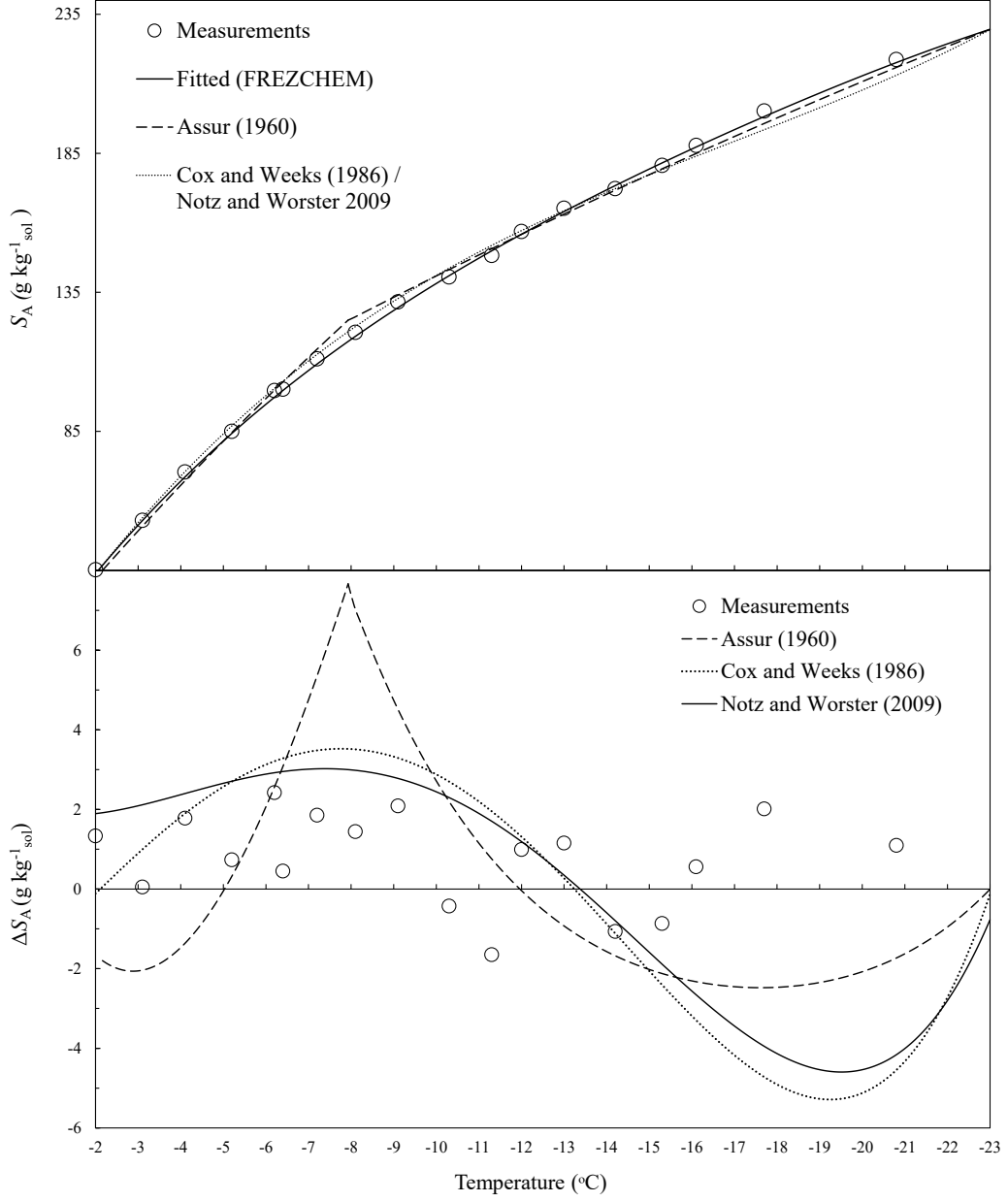


Figure 3: Top: A comparison of the refined $S_A - T_{\text{fr}}$ relationship (equation 7) with that of Assur (1960), Cox and Weeks (1986), and Notz and Worster (2009). Bottom: The ΔS_A of our measurements and other $S_A - T_{\text{fr}}$ equations, when compared to our refined $S_A - T_{\text{fr}}$ relationship of equation 7.

389 Further differences at approximately $-19\text{ }^{\circ}\text{C}$, most notably with respect to
 390 the equations of Cox and Weeks (1986) and Notz and Worster (2009), are
 391 observed due to inaccuracies in fitting the Assur (1960) data to a single
 392 polynomial function. Compared to our refined $S_A - T_{\text{fr}}$ relationship of sea ice
 393 brines (equation 7), the previous equations over-estimate S_A by the greatest
 394 extent at $-8\text{ }^{\circ}\text{C}$ ($3.1 - 7.7\text{ g kg}_{\text{sol}}^{-1}$) and underestimate it by $2.5 - 5.3\text{ g kg}_{\text{sol}}^{-1}$
 395 below $-17\text{ }^{\circ}\text{C}$ (figure 3, bottom). The average error (ΔS_A) of our S_A^{meas}
 396 relative to equation 7 is $1.38\text{ g kg}_{\text{sol}}^{-1}$, compared to ΔS_A of 3.10, 3.14 and 2.83
 397 $\text{g kg}_{\text{sol}}^{-1}$ relative to the equations of Assur (1960), Cox and Weeks (1986), and
 398 Notz and Worster (2009), respectively.

399 The precipitation of ikaite and gypsum from sea ice brines could affect the
 400 accuracy of our refined $S_A - T_{\text{fr}}$ relationship. Using the highest available esti-
 401 mates for the extent of ikaite and gypsum precipitation outlined in section 3,
 402 the combined effect of their precipitation could decrease S_A by $0.02\text{ g kg}_{\text{sol}}^{-1}$
 403 at $-2\text{ }^{\circ}\text{C}$ and $0.47\text{ g kg}_{\text{sol}}^{-1}$ at $-22.8\text{ }^{\circ}\text{C}$. Compared to the changes induced
 404 by mirabilite precipitation, the potential effect of ikaite and gypsum is low.
 405 This analysis therefore indicates that incorporating up-to-date information
 406 about mirabilite dynamics (Butler et al., 2016) into the $S_A - T_{\text{fr}}$ relationship
 407 of equilibrium sea ice brines results in a more accurate description of brine
 408 salinities. The reduction in error compared to previous liquidus equations
 409 can be attributed to experimental and analytical limitations in the original
 410 investigation of Nelson and Thompson (1954), mainly relating to insufficient
 411 mirabilite equilibration in their experiments (Butler et al., 2016).

4.2. *The practical salinity–temperature relationship in sea ice brines*

Practical salinity is the property measured in sea ice field studies where it is almost exclusively assumed that $S_P = S_A$ (Gleitz et al., 1995; Krembs et al., 2000; Papadimitriou et al., 2004; Munro et al., 2010; Norman et al., 2011). This assumption is reasonable for brines that retain the ionic stoichiometry of Standard Seawater (table 1). However, it is now evident that the S_A/S_P of Standard Seawater is compromised in sea ice brines below -6.4 °C due to mirabilite precipitation. Our measured and modelled results indicate that S_P increases at a greater rate than S_A between -6.4 and -22.8 °C, approaching differences of >7 % as the temperature decreases (figures 1 and 2). This deviation substantiates the need for careful consideration of the S_A/S_P relationship in research involving sea ice brines with salinity measured on the practical scale as per typical field sampling protocols.

Existing state equations are related to S_A rather than S_P (section 4.1), which is not representative of the method by which sea ice brine salinity is currently measured in the field. Therefore, similarly to the $S_A - T_{\text{fr}}$ relationship for sea ice brines, an $S_P - T_{\text{fr}}$ relationship, implicit of mirabilite precipitation, can also be derived from this investigation. Owing to the accuracy of S_P^{mod} compared to our measurements (section 3), we fitted the modelled results between -1.8 and -22.8 °C first to an equation that yields S_P as a function of ice temperature T (°C) at ice-brine equilibrium:

$$S_P(T_{\text{fr}}) = 2.6105 - 18.8791T_{\text{fr}} - 0.5193T_{\text{fr}}^2 - 0.0070T_{\text{fr}}^3, \quad (9)$$

with $R^2 = 0.99998$, $\sigma = 0.295$, $n = 211$ and $p < 0.001$. Secondly, we derive an equation describing the brine freezing point (T_{fr}) as a function of S_P ,

435 where

$$T_{\text{fr}}(S_{\text{P}}) = 0.3145 - 0.0605S_{\text{P}} + 3.1575 \times 10^{-5}S_{\text{P}}^2 - 6.7696 \times 10^{-7}S_{\text{P}}^3, \quad (10)$$

436 with $R^2 = 0.99999$, $\sigma = 0.016$, $n = 211$ and $p < 0.001$. Equation 10 can be
437 used to accurately calculate the brine freezing point when only S_{P} data is
438 available, which is typically the case for sea ice brines in field studies.

439 The $S_{\text{P}} - T_{\text{fr}}$ (equation 9) and $S_{\text{A}} - T_{\text{fr}}$ (equation 7) relationships are com-
440 pared to available sea ice brine $S_{\text{P}} - T_{\text{fr}}$ data from the field (section 2.5) in
441 figure 4. Between -2 and -6 °C, the field data follow our $S_{\text{P}} - T_{\text{fr}}$ and $S_{\text{A}} - T_{\text{fr}}$
442 relationships as would be expected while conservative physical concentration
443 of seawater ions during freezing keeps the $S_{\text{A}}/S_{\text{P}}$ relationship constant and
444 close to that of Standard Seawater. Below -7 °C the field brine S_{P} contin-
445 ues to increase at a greater rate than our $S_{\text{A}} - T_{\text{fr}}$ relationship, consistent
446 with the divergence of S_{P} and S_{A} as a result of mirabilite-brine equilibrium.
447 The field data are more accordant with our $S_{\text{P}} - T_{\text{fr}}$ relationship that is im-
448 plicit of mirabilite precipitation but the field brine S_{P} increases at a slightly
449 greater rate than our $S_{\text{P}} - T_{\text{fr}}$ relationship at temperatures below -9 °C.
450 This difference may reflect the precipitation of other salts within the field
451 brines (section 3) combined with their more complex solution composition.
452 The discrepancies provide scope for further laboratory or field investigations
453 with natural sea ice brines that may be able to account for these additional
454 dynamics.

455 Norman et al. (2011) discuss that their measurements (figure 4), spanning
456 from -1.3 to -12.4 °C ($n = 184$), evidently fit the empirical equation given

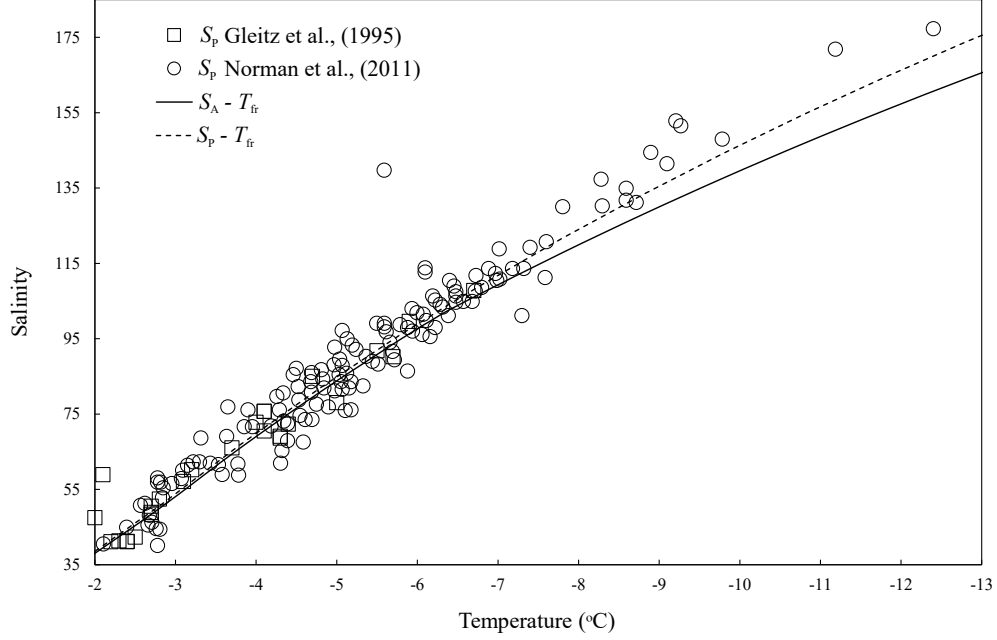


Figure 4: The S_P of natural sea ice brines, taken from Gleitz et al. (1995) and Norman et al. (2011), compared to our $S_A - T_{fr}$ (equation 7) and $S_P - T_{fr}$ (equation 9) relationships.

457 in Assur (1960),

$$S_A = 1000 \left(1 - \frac{54.11}{T} \right)^{-1}, \quad (11)$$

458 which, as explicitly stated by Assur (1960), is only valid for use in sea ice
 459 brines down to -8°C , prior to the onset of mirabilite precipitation. It would
 460 therefore not be expected for the field sea ice brine data to follow equation 11,
 461 unless the brine remained strongly supersaturated with respect to mirabilite,
 462 which is seemingly unlikely given its rapid change in solubility between -6
 463 and -12°C (Butler et al., 2016). Our data analysis instead indicates that
 464 the S_P measured in field sea ice brines obeys a similar $S_P - T_{fr}$ relationship to

465 that of equation 9 due to mirabilite precipitation and its consequent effect on
 466 brine composition. Whilst there are no measurements of S_A in natural sea ice
 467 brines that can be sourced for a direct comparison with the S_P measurements
 468 from the literature, all available data suggests that the universal assumption
 469 of an $S_A - S_P$ equivalence in sea ice brines is inaccurate in the region of
 470 mirabilite precipitation (≤ -6.4 °C).

471 The effect of using the easily measurable S_P instead of S_A for the cal-
 472 culation of brine density (ρ_b), brine volume fraction (v_b/v), brine freezing
 473 point, and the conversion factor (θ) between $\text{mol kg}_{\text{H}_2\text{O}}^{-1}$ and $\text{mol kg}_{\text{sol}}^{-1}$ at
 474 -22.8 °C were evaluated here (table 4). All the differences (Δ) stem from
 475 the divergence of S_P from S_A displayed in figures 1 and 2, which deviate by
 476 7.2 % at -22.8 °C. In relation to the sea ice properties, use of S_P results
 477 in a 13.26 kg m^{-3} overestimation of the brine density and an underestima-
 478 tion of brine volume fraction by 0.0027 (7.8 %). These differences, combined
 479 with a 3.15 °C underestimation of brine T_f upon use of S_P highlight how
 480 any calculation of sea ice properties requires careful consideration of salinity,
 481 while the equivalence of S_A and S_P cannot be relied upon when dealing with
 482 non-conservative sea ice brines. Lastly, the use of S_P in calculation of θ , the
 483 concentration conversion factor, results in a 2.15 % underestimation of con-
 484 centrations. Such differences could easily result in considerable inaccuracies
 485 when converting concentration units for use in thermodynamic models, such
 486 as FREZCHEM, or in models of ionic molal conductivities (McCleskey et al.,
 487 2012).

Table 4: The effect of using S_P rather than S_A ($\text{g kg}_{\text{sol}}^{-1}$) measurement upon the calculation of key physical sea ice parameters at -22.8 °C, with an idealised bulk sea ice S_A of $10 \text{ g kg}_{\text{sol}}^{-1}$.

	Brine	ρ_b^a	$\frac{v_b}{v}^b$	T_{fr}^c	θ^d
	Salinity	kg m^{-3}		°C	
S_A	229.71	1183.77	0.0314	-22.76	0.7703
S_P	246.28	1197.02	0.0341	-25.91	0.7537
$\Delta(S_A - S_P)$	-16.57	-13.26	0.0027	3.15	0.0166
$\Delta S_A(\%)$	-7.21	-1.12	7.7900	-13.84	2.1511

^a $\rho_b = 1000(1 + 0.0008S_A)$ (Cox and Weeks, 1986)

^b $\frac{v_b}{v} = \frac{\rho_{\text{si}}S_{\text{si}}}{\rho_b S_A}$ (Cox and Weeks, 1983) where ρ_{si} is sea ice density (fixed at 0.926 g cm^{-3}) and S_{si} is the bulk sea ice salinity.

^c Equation 7

^d $\theta = 1 - 0.001S_A$ (Mucci, 1983)

488 4.3. Estimating absolute salinity from practical salinity

489 To facilitate a more accurate description of *in-situ* sea ice properties,
490 we formulated a conversion factor (Φ), which may be used to estimate S_A
491 from measurement of S_P in natural sea ice brines (S_P^{nat}) within the range
492 of mirabilite precipitation. We assume that $S_A = S_P$ prior to mirabilite
493 precipitation ($T > -6.4$ °C). For temperatures between -6.4 and -22.8 °C
494 (brine S_P between 103 and 246), we derive Φ using S_P^{mod} and S_A^{mod} . We

495 hence defined Φ as:

$$\Phi = \frac{S_A^{\text{mod}}}{S_P^{\text{mod}}}, \quad (12)$$

496 which was fitted to a third order polynomial function of S_P^{mod} ($R^2 = 0.99997$,
497 $\sigma = 0.0004$, $n = 165$, $p < 0.001$):

$$\Phi(S_P) = 1.2090 - 3.4967 \times 10^{-3} S_P + 1.538 \times 10^{-5} S_P^2 - 2.333 \times 10^{-8} S_P^3. \quad (13)$$

498 By calculating Φ from equation 13, the S_P of sea ice brines measured in the
499 field (S_P^{nat}) may then be converted to an estimate of absolute salinity, S_A^{conv} ,
500 by

$$S_A^{\text{conv}} = S_P^{\text{nat}} \Phi. \quad (14)$$

501 Equation 13 was used to derive Φ for values of S_P^{nat} ranging from 103 to 177
502 extracted from Norman et al. (2011), and hence estimate S_A^{conv} (figure 5).
503 The results show how Φ can aid in accounting for the effects of mirabilite
504 precipitation on the salinity of sea ice brines, providing an estimate of S_A ,
505 whilst still exploiting the practical advantages of S_P measurement in the
506 field. Use of Φ within this range approximately halved the average error of
507 available data, relative to S_A (equation 7), from 6.81 ± 5.36 %, to 3.49 ± 4.15 %.
508 Despite this improvement, Φ does not fully account for the difference between
509 the measured S_P of natural brines in the field (figure 5) and the $S_A - T_{\text{fr}}$
510 relationship of equation 7. At present there are no measurements of sea ice
511 brine S_A from the field, therefore current work is reliant upon the assumption
512 that the brines are at thermal and chemical equilibrium. Additionally, the
513 improved understanding of S_A and S_P in sea ice brines from this investigation
514 cannot account for potential effects from the more complex composition of
515 natural brines and the potential precipitation of ikaite and gypsum.

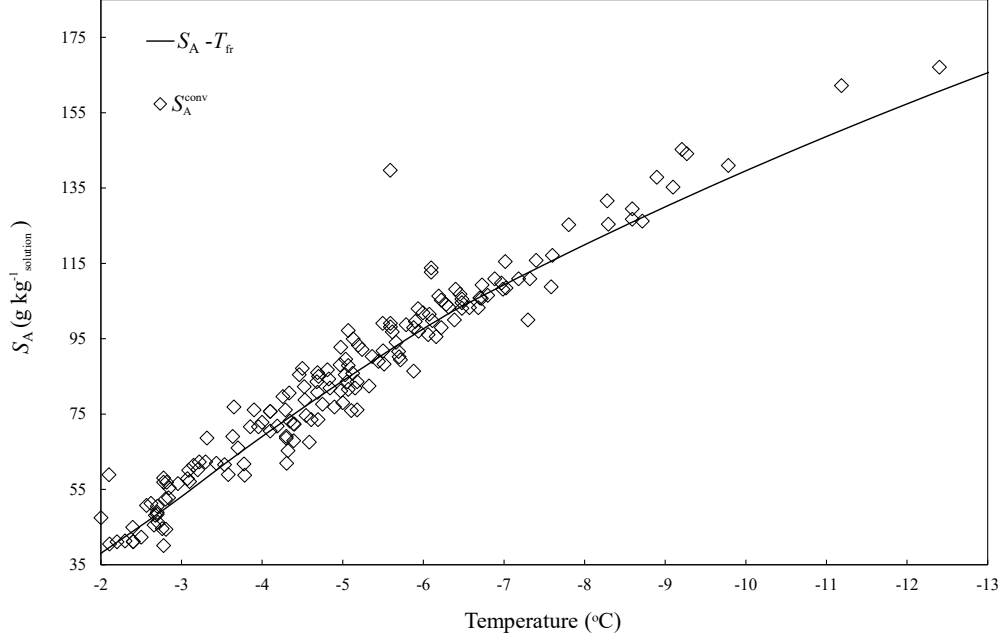


Figure 5: The S_A^{conv} of natural sea ice brines versus brine temperature. The S_A^{conv} was computed from S_P measurements in field samples of sackhole brines using equations 13 and 14. The field $S_P - T_{\text{fr}}$ data were taken from Gleitz et al. (1995) and Norman et al. (2011). The solid line represents the refined $S_A - T_{\text{fr}}$ equation of this study (equation 7).

4.4. The Density Salinity of sea ice brines

Methods of quantifying salinity are continuously developing in order to obtain the most accurate and reproducible measurements in aquatic environments. Since the introduction of PSS-78, the measurement of S_P has dominated oceanography at sea and in the laboratory. Here, it was shown that S_P is an unsuitable measure of salinity in sea ice brines when mirabilite precipitation causes non-conservative behaviour of Na^+ and SO_4^{2-} .

When PSS-78 was developed, conductivity was the conservative property of seawater that could be measured with the greatest accuracy and repro-

ducibility (Lewis, 1980). However, with recent advances in optical salinity sensors (Grosso et al., 2010), it is now also possible to measure the density of solutions very accurately, rapidly, and in an SI-traceable manner (IOC et al., 2010). Measurement of solution density can then be used to accurately determine S_A (Naftz et al., 2011). The most recent Thermodynamic Equation of Seawater 2010 (TEOS-10) computes S_A from the measurement of solution density, thus deriving ‘Density Salinity’ (S_A^{dens}) and decreasing the reliance upon conductivity-based salinity (IOC et al., 2010; Wright et al., 2011). The S_A^{dens} is the value of absolute salinity that is derived from the solution density at 25 °C and 0 dbar pressure. Whilst S_A^{dens} is defined for seawater in TEOS-10 (IOC et al., 2010), a similar protocol can be employed that is specific to sea ice brines, thus allowing S_A^{dens} determination from measurement of sea ice brine density.

The FREZCHEM code, shown to be accurate in the computation of S_A in sea ice brines, also computes brine density and hence can define the S_A^{dens} of this system. The accuracy of FREZCHEM for computing solution density can be shown from its output for Standard Seawater ($S_A = 35.157 \text{ g kg}_{\text{sol}}^{-1}$) at 25 °C and 0 dbar pressure. FREZCHEM computes a density of $1023.356 \text{ kg m}^{-3}$, which is within 0.002 % of the value of $1023.334 \pm 0.0036 \text{ kg m}^{-3}$ derived from the seawater density equation of Millero and Huang (2009). Following the IOC protocol, sea ice brine densities were computed by FREZCHEM at 25 °C and 0 dbar for the solution compositions that were used to calculate S_A^{mod} between -1.8 and -22.8 °C (section 2.3). From this, S_A^{dens} ($\text{g kg}_{\text{sol}}^{-1}$), which is equivalent to S_A^{mod} , can be described by a third order polynomial function of brine density ρ_b (kg m^{-3}) ($R^2 = 0.99999$, $\sigma = 0.176$, $p < 0.001$,

550 $n = 85$):

$$S_A^{\text{dens}} = 4.36370 \times 10^3 - 14.59216 \rho_b + 1.48655 \times 10^{-2} \rho_b^2 - 4.63118 \times 10^{-6} \rho_b^3. \quad (15)$$

551 The above $S_A^{\text{dens}} - \rho_b$ relationship links this work to the current description
552 of salinity in the TEOS-10 standards of practice. This approach is already
553 employed for salinity measurements in hypersaline lakes (Naftz et al., 2011;
554 Anati, 1999), hence the measurement of solution density at 25 °C rather than
555 conductivity can be included in the sea ice standards of practice protocol as a
556 reliable method for quantifying the salinity of sea ice brines. The assessment
557 of S_A and S_P in this work offers a more comprehensive understanding of sea
558 ice brine salinity, reliable means of determining it accurately, and guidelines
559 for the improvement of field and laboratory measurements, all in line with
560 current practice in oceanography. The caveat at present, however, is that
561 the equations in this study are based on modelled synthetic brines with a
562 simplified composition relative to that of brines in a natural sea ice system.
563 Until measurements of natural brine S_A and density are made, the data and
564 equations provided here for a simplified synthetic system remain the best
565 available measure of sea ice brine salinities to -22.8 °C in the presence of
566 mirabilite. For these reasons, future field work should include measurement of
567 brine density and S_A along with the standard measurements of conductivity-
568 based S_P to align the field of high latitude oceanic biogeochemistry with
569 standard oceanographic practices (IOC et al., 2010).

570 5. Conclusions

571 Measurements and modelling of the ionic composition and electrical con-
572 ductivity of synthetic sea ice brines between -1.8 and -22.8 °C have revealed

573 how mirabilite precipitation below $-6.4\text{ }^{\circ}\text{C}$ affects the S_A and S_P of the brine
 574 to a measurable, and different, extent for each parameter. We have first re-
 575 fined the $S_A - T_{\text{fr}}$ relationship for sea ice brines to account for the new and
 576 comprehensive information about mirabilite precipitation in sea ice brines.
 577 Furthermore, the first $S_P - T_{\text{fr}}$ relationship has been formulated for sea ice
 578 brines at thermal equilibrium. Our analysis has shown that, between -6.4
 579 and $-22.8\text{ }^{\circ}\text{C}$, the S_P increases at a greater rate than S_A due to the redis-
 580 tribution of individual ion contributions to the total electrical conductivity
 581 of the solution and the total concentration of dissolved salts. As a result, it
 582 is highlighted that the widespread assumption of S_A and S_P equivalence in
 583 sea ice brines incurs and propagates errors in the calculation of key physi-
 584 cal parameters of the sea ice system, whilst misrepresenting the conditions
 585 inhabited by sympagic organisms. Existing data of field sea ice brine S_P
 586 from the Southern Ocean is in agreement with our modelled and measured
 587 data from synthetic seawater brines. We therefore propose that the observed
 588 $S_P - T_{\text{fr}}$ relationship in natural sea ice brines is a reflection of mirabilite
 589 precipitation in the field temperature region where this reaction is expected
 590 to occur ($T \leq -6.4\text{ }^{\circ}\text{C}$). The ease with which electrical conductivity can be
 591 measured for S_P determination will likely cement its use in field investiga-
 592 tions for years to come. We have therefore formulated a conversion factor
 593 for estimation of S_A from measurement of S_P in sea ice brines affected by
 594 mirabilite precipitation. To help progress towards a description of sea ice
 595 brine salinity that is aligned with the most recent oceanography standard,
 596 TEOS-10, we have also formulated a relationship between absolute salinity
 597 and brine density.

598 The equations maintain the current paradigm that brines attain ther-
599 mal and chemical equilibrium, and could be further refined with additional
600 investigations using naturally derived seawater brines. Similar work in the
601 coldest temperature region of sea ice, between -23°C and the eutectic,
602 where other minerals are understood to precipitate and interact, could aid
603 in developing an accurate understanding of salinity in such hypersaline and
604 non-conservative conditions.

605 **6. Acknowledgements**

606 The work was supported by a NERC Algorithm Studentship (NE/K501013),
607 beamtime awards EE-3897-1 and EE-12301-1 from Diamond Light Source
608 Ltd, and a PhD Student Grant from the International Association of Geo-
609 chemistry. We are very thankful to the I11 beamline team, Professor Chiu
610 Tang, Dr Sarah Day and Dr Claire Murray for their support during beam-
611 time. The generosity of advice and resources from Dr Vera Thoss in the
612 School of Chemistry, Bangor University, was invaluable throughout this in-
613 vestigation. We also thank the three anonymous reviewers for their construc-
614 tive comments, which helped to improve this paper. All data presented here
615 are freely available upon contacting the corresponding author.

616 **References**

- 617 Anati, D. A., 1999. The salinity of hypersaline brines: concepts and miscon-
618 ceptions. *International Journal of Salt Lake Research* 8 (1), 55–70.
- 619 Assur, A., 1960. Composition of sea ice and its tensile strength. Tech. rep.,

620 44, Arctic Sea Ice, U.S. National Academy of Sciences, National Research
621 Council, U.S.A.

622 Butler, B. M., Kennedy, H., 2015. An investigation of mineral dynamics in
623 frozen seawater brines by direct measurement with synchrotron X-ray pow-
624 der diffraction. *Journal of Geophysical Research: Oceans* 120 (8), 5686–
625 5697.

626 Butler, B. M., Papadimitriou, S., Santoro, A., Kennedy, H., 2016. Mirabilite
627 solubility in equilibrium sea ice brines. *Geochimica et Cosmochimica Acta*
628 182, 40 – 54.

629 Collins, R. E., Carpenter, S. D., Deming, J. W., 2008. Spatial heterogeneity
630 and temporal dynamics of particles, bacteria, and pEPS in Arctic winter
631 sea ice. *Journal of Marine Systems* 74 (3), 902–917.

632 Cox, G. F. N., Weeks, W. F., 1983. Equations for determining the gas and
633 brine volumes in sea ice samples. *Journal of Glaciology* 29 (102), 306–316.

634 Cox, G. F. N., Weeks, W. F., 1986. Changes in the salinity and porosity
635 of sea-ice samples during shipping and storage. *Journal of Glaciology* 32,
636 371–375.

637 Cox, G. F. N., Weeks, W. F., 1988. Numerical simulations of the profile prop-
638 erties of undeformed first-year sea ice during the growth season. *Journal*
639 *of Geophysical Research: Oceans* 93 (C10), 12449–12460.

640 Dieckmann, G. S., Hellmer, H. H., 2010. The importance of sea ice: An
641 overview. *Sea Ice* 2, 1–22.

642 Dieckmann, G. S., Nehrke, G., Papadimitriou, S., Göttlicher, J., Steininger,
 643 R., Kennedy, H., Wolf-Gladrow, D., Thomas, D. N., 2008. Calcium car-
 644 bonate as ikaite crystals in Antarctic sea ice. *Geophysical Research Letters*
 645 35 (8), L08501.

646 Dittmar, W., Thomson, C., Buchanan, J., 1873. Report on Researches Into
 647 the Composition of Ocean-Water. Report on the scientific results of the
 648 voyage of H.M.S. Challenger during the years 1873-1876. Physics and chem-
 649 istry.

650 DOE, 1994. Handbook of methods for the analysis of the various parameters
 651 of the carbon dioxide system in sea water; version 2. A. G. Dickson & C.
 652 Goyet ORNL/CDIAC.

653 Ewert, M., Deming, J. W., 2013. Sea ice microorganisms: Environmental
 654 constraints and extracellular responses. *Biology* 2 (2), 603–628.

655 Fischer, M., Thomas, D. N., Krell, A., Nehrke, G., Göttlicher, J., Norman, L.,
 656 Meiners, K. M., Riaux-Gobin, C., Dieckmann, G. S., 2013. Quantification
 657 of ikaite in Antarctic sea ice. *Antarct. Sci* 25 (3), 421–432.

658 Fofonoff, N., 1985. Physical properties of seawater: A new salinity scale and
 659 equation of state for seawater. *Journal of Geophysical Research: Oceans*
 660 (1978–2012) 90 (C2), 3332–3342.

661 Forchhammer, G., 1865. On the composition of sea-water in the different
 662 parts of the ocean. *Philosophical Transactions of the Royal Society of Lon-*
 663 *don* 155, 203–262.

- 664 Garrison, D. L., Jeffries, M. O., Gibson, A., Coale, S. L., Neenan, D., Fritsen,
665 C., Okolodkov, Y. B., Gowing, M. M., 2003. Development of sea ice mi-
666 crobial communities during autumn ice formation in the Ross Sea. *Marine*
667 *Ecology Progress Series* 259, 1–15.
- 668 Geilfus, N.-X., Galley, R. J., Cooper, M., Halden, N., Hare, A., Wang, F.,
669 Sogaard, D. H., Rysgaard, S., 2013. Gypsum crystals observed in experi-
670 mental and natural sea ice. *Geophysical Research Letters* 40 (24), 6362–
671 6367.
- 672 Gitterman, K. E., 1937. Thermal analysis of seawater. Tech. rep., CRREL
673 TL287, USA Cold Region Research and Engineering Laboratory, Hanover,
674 N.H.
- 675 Gleitz, M., vd Loeff, M. R., Thomas, D. N., Dieckmann, G. S., Millero,
676 F. J., 1995. Comparison of summer and winter inorganic carbon, oxygen
677 and nutrient concentrations in Antarctic sea ice brine. *Marine Chemistry*
678 51 (2), 81–91.
- 679 Golden, K. M., Eicken, H., Heaton, A. L., Miner, J., Pringle, D. J., Zhu,
680 J., 2007. Thermal evolution of permeability and microstructure in sea ice.
681 *Geophysical Research Letters* 34, L16501.
- 682 Grasby, S. E., Rod Smith, I., Bell, T., Forbes, D. L., 2013. Cryogenic forma-
683 tion of brine and sedimentary mirabilite in submergent coastal lake basins,
684 Canadian Arctic. *Geochimica et Cosmochimica Acta* 110, 13–28.
- 685 Grosso, P., Le Menn, M., De La, J.-L. D. B., Wu, Z. Y., Malardé, D.,
686 et al., 2010. Practical versus absolute salinity measurements: New ad-

687 vances in high performance seawater salinity sensors. *Deep Sea Research*
 688 *Part I: Oceanographic Research Papers* 57 (1), 151–156.

689 He, S., Morse, J. W., 1993. The carbonic acid system and calcite solubility
 690 in aqueous Na-K-Ca-Mg-Cl-SO₄ solutions from 0 to 90 °C. *Geochimica et*
 691 *Cosmochimica Acta* 57 (15), 3533–3554.

692 Horner, R., Ackley, S. F., Dieckmann, G. S., Gulliksen, B., Hoshiai, T.,
 693 Legendre, L., Melnikov, I. A., Reeburgh, W. S., Spindler, M., Sullivan,
 694 C. W., 1992. Ecology of sea ice biota. *Polar Biology* 12 (3-4), 417–427.

695 Howarth, R. W., 1978. A rapid and precise method for determining sulfate
 696 in seawater, estuarine waters, and sediment pore waters. *Limnology and*
 697 *Oceanography* 23 (5), 1066–1069.

698 IOC, SCOR, IAPSO, 2010. The international thermodynamic equation of
 699 seawater–2010: Calculation and use of thermodynamic properties. Tech.
 700 rep., Intergovernmental Oceanographic Commission, Manuals and Guides
 701 No. 56 (UNESCO).

702 Jackett, D. R., McDougall, T. J., Feistel, R., Wright, D. G., Griffies, S. M.,
 703 2006. Algorithms for density, potential temperature, conservative temper-
 704 ature, and the freezing temperature of seawater. *Journal of Atmospheric*
 705 *and Oceanic Technology* 23 (12), 1709–1728.

706 Kester, D. R., Duedall, I. W., Connors, D. N., Pytkowicz, R. M., 1967.
 707 Preparation of artifical seawater. *Limnology and Oceanography* 12 (1),
 708 176–179.

- 709 King, B. A., Firing, E., Joyce, T. M., 2001. Ocean Circulation and Climate:
710 Observing and Modelling the Global Ocean. International geophysics se-
711 ries. Academic Press, San Fransisco CA, USA, Ch. Shipboard observations
712 during WOCE.
- 713 Krembs, C., Gradinger, R., Spindler, M., 2000. Implications of brine chan-
714 nel geometry and surface area for the interaction of sympagic organisms
715 in Arctic sea ice. *Journal of Experimental Marine Biology and Ecology*
716 243 (1), 55–80.
- 717 Lewis, E., 1980. The practical salinity scale 1978 and its antecedents. *IEEE*
718 *Journal of Oceanic Engineering* 5 (1), 3–8.
- 719 Light, B., Brandt, R. E., Warren, S. G., 2009. Hydrohalite in cold sea ice:
720 Laboratory observations of single crystals, surface accumulations, and mi-
721 gration rates under a temperature gradient, with application to Snowball
722 Earth. *Journal of Geophysical Research* 114 (C7), C07018.
- 723 Light, B., Maykut, G. A., Grenfell, T. C., 2003. Effects of temperature on the
724 microstructure of first-year Arctic sea ice. *Journal of Geophysical Research*
725 108 (C2), 3051.
- 726 Marion, G. M., Farren, R. E., Komrowski, A. J., 1999. Alternative pathways
727 for seawater freezing. *Cold Regions Science and Technology* 29, 259–266.
- 728 Marion, G. M., Kargel, J. S., 2008. Cold Aqueous Planetary Geochemistry
729 with FREZCHEM. Springer, Heidelberg.
- 730 Marion, G. M., Mironenko, M. V., Roberts, M. W., 2010. FREZCHEM: A

731 geochemical model for cold aqueous solutions. *Computers & Geosciences*
732 36, 10–15.

733 McCaffrey, M., Lazar, B., Holland, H., 1987. The evaporation path of sea-
734 water and the coprecipitation of Br^- and K^+ with halite. *Journal of Sedi-*
735 *mentary Research* 57 (5), 928–937.

736 McCleskey, R. B., Nordstrom, D. K., Ryan, J. N., Ball, J. W., 2012. A new
737 method of calculating electrical conductivity with applications to natural
738 waters. *Geochimica et Cosmochimica Acta* 77, 369 – 382.

739 Miller, L. A., Papakyriakou, T. N., Collins, R. E., Deming, J. W., Ehn, J. K.,
740 Macdonald, R. W., Mucci, A., Owens, O., Raudsepp, M., Sutherland, N.,
741 2011. Carbon dynamics in sea ice: A winter flux time series. *Journal of*
742 *Geophysical Research: Oceans* 116 (C2), c02028.

743 Millero, F. J., Feistel, R., Wright, D. G., McDougall, T. J., 2008. The
744 composition of Standard Seawater and the definition of the Reference-
745 Composition Salinity Scale. *Deep Sea Research Part I* 55, 50–72.

746 Millero, F. J., Huang, F., 2009. The density of seawater as a function of
747 salinity (5 to 70 g kg⁻¹) and temperature (273.15 to 363.15 K). *Ocean*
748 *Science* 5 (2), 91–100.

749 Millero, F. J., Leung, W. H., 1976. The thermodynamics of seawater at one
750 atmosphere. *American Journal of Science* 276 (9), 1035–1077.

751 Mucci, A., 1983. The solubility of calcite and aragonite in seawater at vari-
752 ous salinities, temperatures, and one atmosphere total pressure. *American*
753 *Journal of Science* 283, 780–799.

- 754 Munro, D. R., Dunbar, R. B., Mucciarone, D. A., Arrigo, K. R., Long,
755 M. C., 2010. Stable isotope composition of dissolved inorganic carbon and
756 particulate organic carbon in sea ice from the Ross Sea, Antarctica. *Journal*
757 *of Geophysical Research: Oceans* 115 (C9), c09005.
- 758 Naftz, D. L., Millero, F. J., Jones, B. F., Green, W. R., 2011. An equation
759 of state for hypersaline water in Great Salt Lake, Utah, USA. *Aquatic*
760 *geochemistry* 17 (6), 809–820.
- 761 Nelson, K. H., Thompson, T. G., 1954. Deposition of salts from sea water by
762 frigid concentration. Tech. rep., 29, Office of Naval Research, Arlington,
763 VA.
- 764 Norman, L., Thomas, D. N., Stedmon, C. A., Granskog, M. A., Papadim-
765 itriou, S., Krapp, R. H., Meiners, K. M., Lannuzel, D., van der Merwe, P.,
766 Dieckmann, G. S., 2011. The characteristics of dissolved organic matter
767 (DOM) and chromophoric dissolved organic matter (CDOM) in Antarc-
768 tic sea ice. *Deep Sea Research Part II: Topical Studies in Oceanography*
769 58 (910), 1075 – 1091.
- 770 Notz, D., Worster, M. G., May 2009. Desalination processes of sea ice revis-
771 ited. *Journal of Geophysical Research* 114, C05006.
- 772 Papadimitriou, S., Kennedy, H., Kattner, G., Dieckmann, G., Thomas,
773 D., 2004. Experimental evidence for carbonate precipitation and CO₂ de-
774 gassing during sea ice formation. *Geochimica et Cosmochimica Acta* 68 (8),
775 1749–1761.

- 776 Papadimitriou, S., Kennedy, H., Kennedy, P., Thomas, D. N., 2013. Ikaite
777 solubility in seawater-derived brines at 1 atm and sub-zero temperatures
778 to 265 K. *Geochimica et Cosmochimica Acta* 109, 241–253.
- 779 Papadimitriou, S., Thomas, D. N., Kennedy, H., Haas, C., Kuosa, H., Krell,
780 A., Dieckmann, G. S., 2007. Biogeochemical composition of natural sea ice
781 brines from the Weddell Sea during early austral summer. *Limnology and*
782 *Oceanography* 52 (5), 1809–1823.
- 783 Pawlowicz, R., 2012. The electrical conductivity of seawater at high temper-
784 atures and salinities. *Desalination* 300, 32 – 39.
- 785 Pawlowicz, R., 2015. The absolute salinity of seawater diluted by riverwater.
786 *Deep Sea Research Part I: Oceanographic Research Papers* 101, 71 – 79.
- 787 Perkin, R. G., Lewis, E. L., 1980. The practical salinity scale 1978: fitting
788 the data. *Oceanic Engineering* 5 (1), 9–16.
- 789 Petrich, C., Eicken, H., 2010. Growth, structure and properties of sea ice.
790 *Sea Ice* 2, 23–77.
- 791 Pitzer, K. S., 1973. Thermodynamics of electrolytes. I. Theoretical basis and
792 general equations. *The Journal of Physical Chemistry* 77 (2), 268–277.
- 793 Thomas, D. N., Dieckmann, G. S., 2002. Antarctic Sea ice-a habitat for
794 extremophiles. *Science* 295, 641–644.
- 795 Thomas, D. N., Papadimitriou, S., Michel, C., 2010. Biogeochemistry of sea
796 ice. *Sea Ice* 2, 425–467.

- 797 Weeks, W., 2010. On Sea Ice. University of Alaska Press.
- 798 Weeks, W. F., Ackley, S. F., 1986. The growth, structure, and properties of
799 sea ice. Springer.
- 800 Wright, D., Pawlowicz, R., McDougall, T., Feistel, R., Marion, G., 2011.
801 Absolute salinity,” density salinity” and the reference-composition salinity
802 scale: present and future use in the seawater standard teos-10. Ocean
803 Science 7 (1), 1–26.